Influence of Knowledge Uncertainties on the Safety Assessment of Existing Post-tensioned Concrete Bridges

Alberto Poeta , Fabio Micozzi * , Laura Gioiella , Andrea Dall'Asta

Posted Date: 6 March 2024

doi: 10.20944/preprints202403.0290.v1

Keywords: Existing post tensioned concrete bridges; Safety format; Monte-Carlo simulation; , Knowledge uncertainties; Semi-Probabilistic approach

 doi:10.20944/preprints202403.0290.v1

Article

Influence of Knowledge Uncertainties on the Safety Assessment of Existing Post-Tensioned Concrete Bridges

Alberto Poeta, Fabio Micozzi *, Laura Gioiella and Andrea Dall'Asta

SAAD School of Architecture and Design, University of Camerino, Viale della Rimembranza 63100 Ascoli Piceno, Italy

* Correspondence: fabio.micozzi@unicam.it; Tel.: +39 3384010779

Abstract: The assessment of existing bridges constitutes a serious challenge for the researchers since their safety evaluation is a complex task due to several sources of uncertainty affecting the parameters identified in the knowledge process. In particular, a high level of uncertainties may arise in the case of prestressing systems requiring special investigation strategies and experimental technologies. The paper aims to investigate how the knowledge uncertainties influence the safety assessment of existing post-tensioned bridges. The semi-probabilistic approach is used, and uncertainties related to the knowledge process are described considering the number of tests, the confidence level assumed for the estimation of the problem parameters, and the measurement errors of in-situ tests. Results concerning a typical post-tensioned bridge are reported and the variability of the outcomes is discussed and compared with a reference case of "perfect knowledge". The main results of the study confirm the general robustness of the semi-probabilistic Eurocodes safety format and provide an overview of dispersion due to different choices about the number of tests and confidence level. The measurement errors may lead to significant under-estimation of the computed structural capacity with respect to the reference one.

Keywords: existing post tensioned concrete bridges; safety format; Monte-Carlo simulation; knowledge uncertainties; semi-probabilistic approach

1. Introduction

Existing bridges constitute a significant portion of the transport infrastructure. A large part of them, although designed according to old Codes, is still in service. Such infrastructures can suffer the effects of both natural hazard (e.g. earthquakes 1 and floods 3) and anthropic loads. It is quite common to find bridges subjected to actions larger than the actions considered in the design, due to the increasing of the total traffic and travelling loads. Furthermore, many bridges have exceeded their design lifetime and some of them show a significant degradation due to environmental effects and, in some cases, to insufficient maintenance interventions. These aspects have been highlighted by the unexpected collapses of bridges occurred worldwide in the recent past, causing economic and social losses. Among them, the collapse of the Fossano overpass in Cuneo in 2016 (IT), the Polcevera viaduct in Genova in 2019 (IT), the Troja footbridge in Prague in 2017 (RC), the Nanfangao bridge in Taiwan in 2019, and the most recent Fern Hollow Bridge in 2022 in Pittsburgh (US).

From the economical point of view, some recent studies have estimated the budget to renovate bridges in different countries. The COST ACTION 345 report 4 estimated a budget of about 400 billion Euros for the replacement costs of one million of existing bridges in the 27 European countries. In 2013 the Federal Highway Administration 5 estimated that approximately the 25 percent of US bridges were either structurally deficient or functionally obsolete; while in the same year the ASCE Infrastructure Report Card 5 estimated that the annual investment necessary for the improvement of US existing bridges was nearly 20 billion dollars. All these aspects stress the urgency of having an efficient and effective evaluation of the structural reliability of existing bridges to give support to

 doi:10.20944/preprints202403.0290.v1

stakeholders in optimizing the maintenance/restoration interventions, and in properly allocating the limited maintenance budgets 6.

In many countries the majority of bridge stock consists of simply supported Prestressed Concrete beams. Among them the Post Tensioned (PT) concrete bridges are a large part of the population, as in the case of Italy 7. They are a critical set since the assessment of their vulnerability is affected by a notable level of uncertainties. Such uncertainties concern the knowledge of the state of conservation of the precompression system, which cannot be investigated through visual inspection or conventional tests. In the US, this aspect is treated by a specific guideline: the Federal Highway Administration-HRT-13-028 8. Such document provides protocols for sampling grout from tendons, and methods for the detection of grout deficiencies with reference to test techniques used in the American context. The guideline provides a rational approach to extract statistically significant number of grout samples to define the corrosion susceptibility and recommendation for repair/rehabilitation procedures. In England, this topic is treated by the Highway England CS 465 9 and CS 464 10. The first document provides a management procedure for risk review, risk assessment and risk management for post-tensioned concrete bridge. The second, contains requirements related to Non-Destructive Testing (NDT) of highways structures. In Italy, a recent guideline 11 introduced a multi-level analysis for the risk assessment of existing bridges. This document suggests the executions of special inspections for PT bridges through a detailed study of the conditions of the post-tensioned cable system, based on the detection and quantification of defects. Data collected from visual inspections and in situ tests, specific for PT cables, are combined for an overall assessment of the pre-stressing system.

In most practical cases, the evaluation of the structural reliability is carried out through the semi-probabilistic approach 12. In this case, the uncertainties concerning the problem are considered through (deterministic) characteristic parameters combined with partial factors, calibrated according to target values of the probability of failure. The partial factors suggested in most of national and international Standards have been developed for the assessment of new structures 12. However, this approach is suitable for existing structures too, and proposals for partial factors have been developed. For example, the Fib 80 code 13, proposes two different partial factor formats, enabling the incorporation of specific reliability-related aspects for not deteriorated existing structures by considering the actual material properties. This way, all prior data collected from existing design specification and/or original design documents can be combined with information provided by material investigation (both non-destructive and destructive tests) and by visual inspections (e.g. 14). An increase in the number of tests and in the confidence level leads to a reduction in the level of uncertainties of the design parameters estimated. However, a large number of tests is not always feasible and a balance between costs and approximation of the safety estimation should be found. In the field of reliability assessment of existing structures, it can be of interest to include time varying phenomena, as ageing, damage, and deterioration; some studies are currently on-going concerning these topics (16).

The outcome of the semi-probabilistic reliability assessment of new structure is a deterministic safety ratio, i.e. the capacity/demand ratio, and it derives from the knowledge of deterministic design parameters, based on statistical properties of the basic variables. On the contrary, in the case of existing structures, the safety ratio becomes an uncertain quantity since the statistical properties of the basic variables are not known in advance and they can only be estimated from a limited amount of information. The study reported in 20 has underscored the significant impact of knowledge uncertainties on the reliability assessment of existing structures. However, no previous studies have examined this effect on PT members, which are characterized by a greater complexity, a higher number of basic variables, and potentially large uncertainties about measurement errors.

In this paper the reliability assessment of existing PT beams is performed by the semi-probabilistic approach, and the influence of the uncertainties affecting the knowledge process on the following statistical distribution of the safety ratio is evaluated and discussed. More precisely, the design parameters required by the semi-probabilistic approach are estimated, based on the outcomes of in-situ inspections and tests. The influence on the statistical distribution of the safety ratio of three

 doi:10.20944/preprints202403.0290.v1

parameters, (i) the number of tests, (ii) the confidence level chosen for the estimation of the design parameters, and (iii) the measure errors related to test techniques, is investigated.

Three different scenarios have been considered. In the first one an ideal condition of "perfect knowledge" is assumed. Safety checks performed in this condition lead to the reference solution of safety ratios, that is assumed as the real one. In the second scenario the knowledge process is considered: the influence of the number of tests on the safety checks is studied, considering also different choices for the confidence level assumed for the estimation of the parameters. In the third scenario, the error affecting the experimental measures is introduced. The probabilistic distribution of the capacity/demand ratio following different choices regarding number of tests, confidence levels and measure uncertainties is obtained using a Monte Carlo simulation, evaluating and discussing the overall probability to observe values larger than the reference one, i.e. values on the un-safe side. Finally, it is worth to recall that this study focuses only on the propagation of uncertainties from the knowledge process towards the estimation of the safety ratio and the results do not depend on the choice of the set of partial factors.

2. Reliability Evaluation and Notation

Reliability assessment is generally based on the definition of a response function (or limit state function) $g(\boldsymbol{x})$: $R^n \rightarrow R$, where $\boldsymbol{x}$ is a vector collecting the so-called basic variables, or state variables (e.g. geometry, material properties, load magnitude and others), strictly necessary to evaluate the performance indicator g. Failure occurs if the response function is below a threshold $\bar{g}$, i.e. $g(\boldsymbol{x}) < \bar{g}$.

Due to different sources of uncertainties 21, the basic variables $\boldsymbol{x}$ are described by a vector of random variables (r.v.) $\boldsymbol{X}$, whose statistical properties are provided by the joint probability distribution function $f_X(\boldsymbol{x})$, so that the failure probability P_f, which is a probabilistic measure of the structural performance 22, can be evaluated by:

$$P_f = \int I(\boldsymbol{x}) f_X(\boldsymbol{x}) d\boldsymbol{x} \tag{1}$$

where the index function $I(\boldsymbol{x})$ in Equation (1) is defined as follows: $I(\boldsymbol{x}) = 1$ if $g(\boldsymbol{x}) < \bar{g}$, otherwise $I(\boldsymbol{x}) = 0$. The system response is satisfactory if $P_f < \bar{P}_f$ in which the target value $\bar{P}_f$, is usually based on the evaluation of economic and social consequences due to failure.

Response function $g(\boldsymbol{x})$ is often expressed by introducing two separate quantities related to the strength of the system $r(\boldsymbol{x})$, and to the effects of the external actions $e(\boldsymbol{x})$, whose most diffused expressions are the safety margin $z(\boldsymbol{x})$, defined by Equation (2), and the safety ratio $y(\boldsymbol{x})$, defined by Equation (3).

$$z(\boldsymbol{x}) = r(\boldsymbol{x}) - e(\boldsymbol{x}) \tag{2}$$

$$y(\boldsymbol{x}) = r(\boldsymbol{x})/e(\boldsymbol{x}) \tag{3}$$

The failure condition is attained when $z < 0$ or $y < 1$.

Given that $\boldsymbol{X}$ is a r.v., previous functions provide r.v. denoted as $G = g(\boldsymbol{X})$, $Z = z(\boldsymbol{X})$, $Y = y(\boldsymbol{X})$. Consequently, using for example the safety margin, the probability of failure P_f can be computed by integrating the probability distribution of Z over the unsafe domain, as shown in Equation (4).

$$P_f = P[Z = R - E < 0] = \int_{-\infty}^{0} f_Z(\boldsymbol{z})\, dz \tag{4}$$

The reliability assessment is often carried out by an approximated approach (the semi-probabilistic formulation 12) deriving from $\boldsymbol{X}$ a set of deterministic "design" parameters $\boldsymbol{\vartheta}_d$ and estimating, through these parameters, the safety ratio as shown in Equation (5). The parameters

 doi:10.20944/preprints202403.0290.v1

$\boldsymbol{\vartheta}_d$ are usually obtained from strength and action descriptors reduced or amplified by calibrated partial factors, in order to obtain probability of failures close to the threshold when

$$y_d(\boldsymbol{\vartheta}_d) = r(\boldsymbol{\vartheta}_d)/e(\boldsymbol{\vartheta}_d) \tag{5}$$

is equal to 1. In the case of existing structures, as those considered in this study, the properties $f_X(\boldsymbol{x})$ of $\boldsymbol{X}$ can be only estimated by a reduced number of imprecise tests. Consequently, using the semi-probabilistic approach, the components of $\boldsymbol{\vartheta}_d$ are no more deterministic values, but they are r.v. $\overline{\boldsymbol{\Theta}}_d$, that collect possible estimations $\overline{\boldsymbol{\vartheta}}_d$ of $\boldsymbol{\vartheta}_d$. For example, the expected variability of $\overline{\boldsymbol{\vartheta}}_d$ reduces by increasing the number of tests. Consequently, the expected safety ratio $\overline{Y}_d = y_d(\overline{\boldsymbol{\Theta}}_d)$ is a r.v. too.

3. Safety Assessment of Existing PT Bridges

As previously stated, the semi-probabilistic approach is used in the following for the safety assessment. First, the basic random variables $\boldsymbol{X}$, chosen in this study to characterize the PT bridge properties are defined, and the related deterministic parameters $\boldsymbol{\vartheta}_d$ required for the safety checks are introduced. Successively, the safety checks with respect to two failure conditions that are mainly influenced by the prestressing system: bending failure and shear failure, are described. Finally, the methods used for the estimation of $\overline{\boldsymbol{\vartheta}}_d$ from experimental tests are discussed.

3.1. Basic Random Variables and Parameters for the Semi-Probabilistic Method

The basic variable vector $\boldsymbol{x}$ generally collects geometrical, mechanical, and material properties. In the problem analysed in this study vector $\boldsymbol{x}$ is defined as follows

$$\boldsymbol{x} = [A_p, P_{pt}, f_{up}, f_{ys}, f_c] \tag{6}$$

where the collected quantities describe the uncertain basic properties of the beam. More in detail A_p denotes the wires area; P_{pt} the current prestressing force; f_{up} the ultimate strength of prestressing steel; f_{ys} the yielding strength of the rebar; and f_c the concrete strength. All the other basic variables (e.g. the beam width, the cable path, and so on), not contained in vector $\boldsymbol{x}$, are assumed as known quantities described by deterministic values.

It is assumed that the components of $\boldsymbol{x}$ are statistically independent. They describe physical quantities that cannot be lower than 0, therefore their probability distribution describing the statistical properties of each random variable is assumed to be log-normal.

The parameters $\boldsymbol{\vartheta}_d$ required in the semi-probabilistic approach based on the partial factors for the safety checks are

$$\boldsymbol{\vartheta}_d = [A_{pm}, P_{pt\_m}, f_{ysd}, f_{upd}, f_{cd}] \tag{7}$$

The vector $\boldsymbol{\vartheta}_d$ encompasses the mean values of the wires area A_{pm}; the mean value of the current prestressing force P_{pt_m}; and the design values of the strength of materials f_{ysd}, f_{upd}, f_{cd} derived by the ratio between their characteristic value and the relevant partial factor.

3.2. Failure Condition Modalities and Safety Checks

The safety checks are carried out by evaluating the safety ratio y_d of Equation (5), using the partial factor method. The considered checks are related to shear and to bending moment; both the failure conditions are considered since they are significantly influenced by the precompression system. The design values of resistances and actions have been computed using the same partial factors γ used for new structures as suggested in 12.

More in detail, the shear is checked at the first cracked section of the beam. The literature provides several studies with refined and complex formulas to predict the shear capacity of prestressed concrete members 23s. In the following, the shear capacity is calculated according to the recommendations proposed by Italian Standard 25 and Eurocode 26 through the formulas for

 doi:10.20944/preprints202403.0290.v1

elements with and without shear-reinforcement. The relative variation is expected to be similar using more refined shear resistance models. In case of shear reinforcement, the shear capacity is derived using the following expressions

$$V_{Rd,1} = min(V_{Rsd}, V_{Rcd}) \tag{8}$$

$$V_{Rsd} = 0.9d\frac{A_{sw}}{s} f_{ysd}(\cot\delta + \cot\vartheta)\sin\delta \tag{9}$$

$$V_{Rcd} = 0.9db_w\alpha_c\upsilon f_{cd}(\cot\delta + \cot\vartheta)/\,(1 + \cot^2\vartheta) \tag{10}$$

where d is the effective height of the cross-section; b_w is the minimum width between tension and compression chord; ϑ is the angle between the concrete compression strut and the beam axis perpendicular to the shear action; δ is the angle between shear reinforcement and the beam axis perpendicular to the shear force; A_{sw} is the cross-sectional area of the shear reinforcement; s is the spacing of the stirrups; f_{ysd} is the design value of the rebar yielding strength obtained as f_{ysk}/γ_s, where γ_s is a partial factor equal to 1.15; α_c is the coefficient taking into account the state of stress in the compression chord; f_{cd} is the design value of the concrete strength obtained as f_{ck}/γ_c, where γ_c is a partial factor equal to 1.5; and υ is the strength reduction factor for concrete cracked in shear. Further information can be found in chapters 4.1.2.3.5.2 of 25 and 6.2.3 of 26.

The shear capacity for unreinforced cracked concrete is calculated trough the following equation.

$$V_{Rd,2} = max\{[C_{Rd,c}\,k(100\rho_1 f_{ck})^{1/3} + k_1\sigma_{cp}]b_w d\,;\,(v_{min} + 0.15\sigma_{cp})b_w d\} \tag{11}$$

where d is the effective height of the cross-section; b_w is the smallest width of the cross-section in tensile area; k is a parameter depending on d; f_{ck} is the characteristic value of the concrete compressive strength; $C_{Rd,c}$ and k_1 are parameters whose values are defined in national annexes, however their recommended values are $0.18/\gamma_c$ and 0.15, respectively; v_{min} is a parameter that depends on f_{ck}, and k; ρ_1 is a ratio depending on the area of tensile reinforcement, b_w, and d; σ_{cp} is the axial stress in the cross section defined as the ratio between the actual prestressing force P_{pt_m}, and the area of concrete A_c of the cross section. Further information can be found in chapter 4.1.2.3.5.1 of 25 and 6.2.2 of 26.

In the case of post-tensioned prestressed elements, the shear contribution given by the vertical component of the prestressing force, V_{cp}, shall be added to obtain the total shear capacity, V_{Rd}. This component can be computed as

$$V_{cp} = P_{pt\_m}\sin\alpha_{cp} \tag{12}$$

where P_{pt_m} is the prestressing force of the cross-section; and α_{cp} is the angle between the prestressing force and the longitudinal axes of the beam. In the shear check the resultant cable is adopted for the prestressing force and its location.

For both the cases, the safety shear ratio $y_{d,s}$ is calculated as follows and its greater value is chosen

$$y_{d,s} = max\left(\frac{V_{cp} + V_{Rd,1}}{V_{ed}}, \frac{V_{cp} + V_{Rd,2}}{V_{ed}}\right) \tag{13}$$

where V_{ed} is the shear action acting on the section under investigation.

In the case of bending check over a generic cross section, the resistant bending moment, M_{Rd}, can be computed as

$$M_{Rd} = Td^* \tag{14}$$

 doi:10.20944/preprints202403.0290.v1

$$T = f_{ypd}A_{pm} + f_{ysd}A_s \tag{15}$$

where T is the resultant tensile force containing the contributions given by the resultant cable, and by the reinforcement steel located under the neutral axis at the ultimate condition; f_{ypd} is the design value of the yielding strength of prestressing steel obtained as f_{ypk}/γ_s; A_s is the area of the reinforcing steel; d^* is the arm between the two resultant compressive and tensile forces. The bending check is usually carried out at the midpoint of the simply supported beam since that section is the most stressed one.

The safety bending ratio is obtained as

$$y_{d,b} = \frac{M_{Rd}}{M_{ed}} \tag{16}$$

where M_{ed} is the design bending moment due to external actions.

A safety check is satisfied if this ratio is equal or greater than 1. Moreover, in this paper the envelope y_d is used, considering both the checks and calculated as

$$y_d = min\left(y_{d,b}, y_{d,s}\right) \tag{17}$$

Previous Equations (10)–(12) and (14) are sensitive to the characteristics of the post-tensioning system that in turn involves the area of the cables A_{pm}, the actual prestressing force P_{pt_m}, and the characteristic yield stress of the harmonic steel f_{ypk}. The resistant bending moment is clearly sensitive to A_{pm} and f_{ypk}, while the shear resistance is, instead, sensitive to the prestressing force. The P_{pt_m} influences Equation (10) through the term α_c representing the compressive state of the section given by the prestressing system, while P_{pt_m} explicitly appears in Equations (11) and (12). Moreover, all the previous parameters indirectly influence the shear capacity because they sway the position of the first cracked section in which V_{cp} is different. By reducing the prestressing action, the first cracked section moves towards the beam support, resulting in a higher V_{ed}.

3.3. Estimation of the Design Parameters Based on Experimental Measurements

The semi-probabilistic method requires that some design parameters ϑ_d of X are estimated from a limited number n of tests providing samples $\bar{x}$. Estimated parameters are r.v. $\bar{\vartheta}_d$ and the confidence $\alpha = P[\bar{\vartheta}_d < \vartheta_d]$ is the probability that the estimated parameter is lower than the actual value. If the Cumulative Density Function (*CDF*) of $\bar{\vartheta}_d$ is available, it is possible to define the limit value $\bar{\vartheta}_d^{\alpha}$ of the estimated quantity, such that $F_{\bar{\vartheta}_d}(\bar{\vartheta}_d^{\alpha}) = \alpha$.

For example, being X a single valued normally distributed r.v. whose standard deviation σ_X is known, it is possible to estimate the mean X_m by the sample mean

$$\bar{x}_m = \frac{1}{n}\sum_{i=1}^{n} x_i \tag{18}$$

The estimation of the mean is a normally distributed r.v., whose expected value is equal to the real mean, $\mu_{\bar{X}} = \mu$, and the standard deviation depends on σ_X and on the number of tests, $\sigma_{\bar{X}_n} = \sigma_X/\sqrt{n}$. Once both mean and standard deviation of $\bar{X}_m$ are known, the probability density function (*pdf*) of $\bar{X}_m$ is known and it is possible to evaluate $\bar{x}_m^{\alpha}$ corresponding to the desired confidence level. Many times, instead, the standard deviation σ_X is not known, and in this case $\bar{X}_m$ is distributed according to a Student's t-Distribution depending on both the sample mean and the sample standard deviation 22.

Furthermore, existing bridges differ from new structures as the data used in their assessment can be related to experimental measurements. Every time a measurement is done, its value is affected by error due to the accuracy of the instrument, the environmental conditions, and the operator execution. Consequently, the measurement error introduces an additional variability of the samples, leading to a higher dispersion in the parameter $\bar{\vartheta}_d$ and to a further dispersion of possible values

 doi:10.20944/preprints202403.0290.v1

caught from the probability distribution of the basic variables. The outcomes of the tests carried out to evaluate the sample x_i is a r.v. X_{err} that can be expressed as

$$X_{err} = x_i \cdot \varepsilon(c_{v_\varepsilon}) \tag{19}$$

where $\varepsilon(c_{v_\varepsilon})$ is a log-normally distributed random variable, having zero as log-mean and coefficient of variation equal to c_{v_ε}.

In conclusion, the distribution of the safety ratio deduced from estimated parameters, is influenced by the effective knowledge of each parameter that, in turn, depends on the number of tests n, the confidence level α assumed in its estimation, and the c_{v_ε} describing the measurement error.

4. Case Study Evaluated through Three Different Knowledge Scenarios

In this chapter, either the adopted methods for the estimation of the set of the parameters $\overline{\boldsymbol{\vartheta}}_d$ from the information received by experimental campaigns, and the way to consider the knowledge uncertainties are showed in an application concerning a real existing PT bridge, by considering different combinations of n, α and c_{v_ε}. First, the case study is introduced, then the three considered knowledge scenarios are described.

4.1. Case Study Features

The case study is a typical post-tensioned bridge (Figure 1), with a simple support static scheme and span length equal to 30 m. The deck is made of 5 cast-in-place prestressed I-beams, a slab of 0.23 m thick, and 5 prestressed crossbeams. The original drawing of the cross section of the bridge is reported in Figure 2. Every beam (Figure 3) is prestressed by 6 cables and each cable is composed of 34 strands with diameters of 7 mm. The prestressing procedure has been carried out in two different construction stages. In the first stage, the 4 lower cables have been tensioned after the curing of beam concrete. Later, after the slab and crossbeam casting, the 2 remaining cables, the upper ones, have been tensioned. The original drawing of the position of the cables along the beam (Figure 4) is reported below. It is important to underline that information about bridge geometry, material characteristics, construction stages, and prestressing force have been derived from both original drawings and design reports. The compressive cubic strength of the concrete used for the beam is R_{ck} = 45 MPa, while the one used for the slab is equal to 40 MPa. FeB44k steel has been used for the rebars. Prestressing strands present a characteristic ultimate strength equal to f_{ptk} = 1800 MPa. Each cable has a cross section area equal to A_p = 12.32 cm^2. The mean value of the prestressing stress applied to the cables is equal to σ_{pt} = 1189.6 MPa.

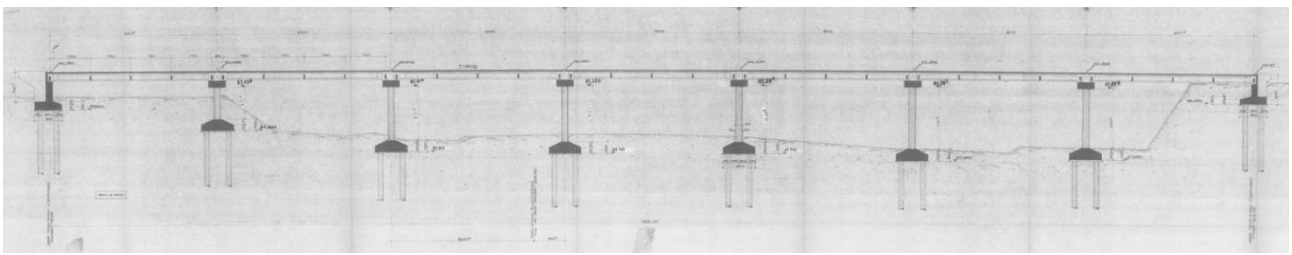

Figure 1. Original longitudinal profile of the bridge.

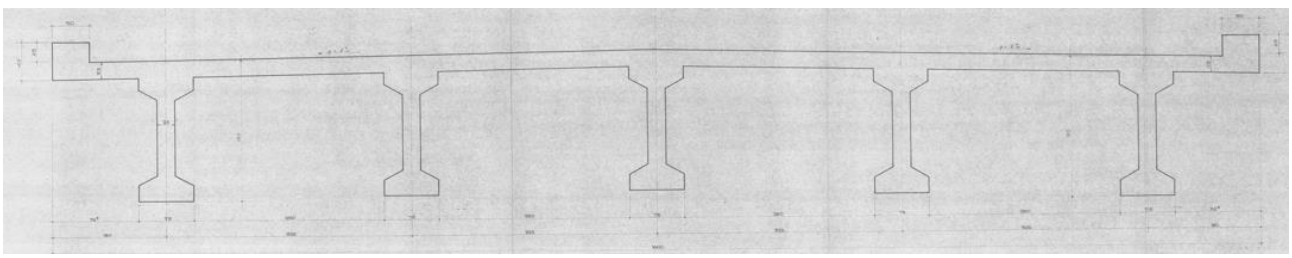

Figure 2. Original cross-section of the bridge deck.

Preprints.org (www.preprints.org) | NOT PEER-REVIEWED | Posted: 6 March 2024 doi:10.20944/preprints202403.0290.v1

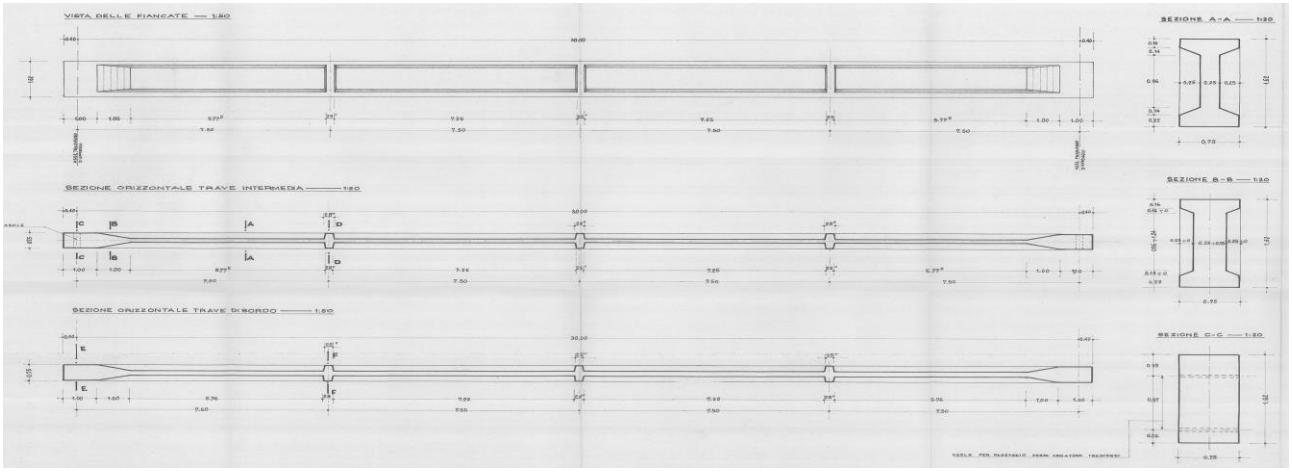

Figure 3. Side, horizontal and cross section original view of the beam.

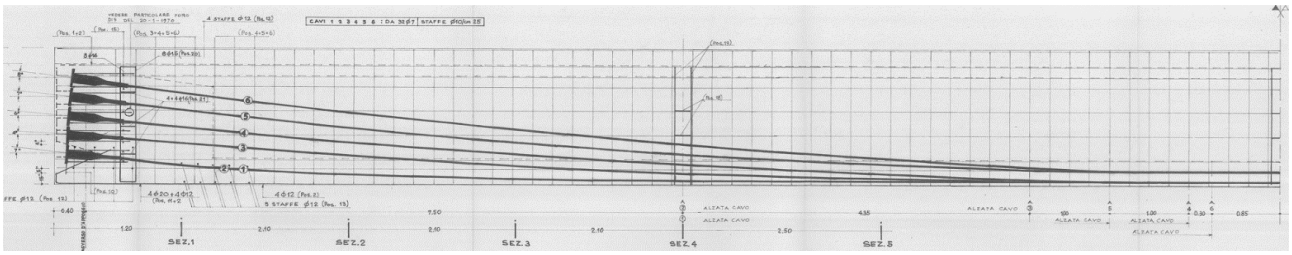

Figure 4. Original location of the strands along the beam.

The actions E_d are evaluated according to 28 (Load Model 1). The SAP2000 29 software has been used to determine the most relevant external effects on the deck. For the safety checks only the most loaded beam is examined.

4.2. Perfect Knowledge Scenario

The perfect knowledge scenario is a theoretical condition that could be hypothetically achieved if an infinite number of tests are carried out, and if test procedures are not affected by errors. In such an ideal scenario, the probability distributions of the basic variables are known and consequently the components of the vector $\boldsymbol{\vartheta}_d$ are deterministic and they can be directly computed from the characteristic values and the partial factors. The characteristic values of the material strengths are calculated as the 5% percentile of their probability distributions, according to the current safety format 12. For what concerns the cables area, the nominal value has been used as suggested by the Standard 12. For what concerns the prestressing action, the Standard 12 recommends using either the mean value P_m or, if relevant, the upper $P_{k,up}$ and lower $P_{k,low}$ characteristic values. In this case, the mean value is adopted. Starting from the initial prestressing force and subtracting the immediate and long-term prestress losses, the nominal value of the prestressing force, is obtained for each cable. The resultant cable force has been computed at all the sections for the safety check calculations.

In this case, the safety ratios ($\gamma_{d,s}$, $\gamma_{d,b}$, γ_d) are deterministic results and they are used for the comparison with the following scenarios simulating the experimental campaigns.

Table 1 shows the probability distributions of $\boldsymbol{X}$ and their related parameters $\boldsymbol{\vartheta}_d$ in the perfect knowledge scenario. The mean values of the geometric basic variable (A_p) and of the strengths of materials (f_c, f_{up}, f_{ys}) are obtained from the information specified in the original technical drawings (terms with the subscript 'op' in Table 1), while their coefficients of variation are acquired from the literature. The mean value of the current prestressing force, P_{pt}, is obtained by subtracting from the initial prestressing force, P_{pt_i}, declared in the original design, the prestress losses ΔP_{pt} (either long-term and immediate ones), calculated following the approach proposed in 26. For P_{pt} a unique coefficient of variation c_{v_p}, is adopted, it includes the uncertainties related to the initial force

 doi:10.20944/preprints202403.0290.v1

applied to the cables, as well as uncertainties related to immediate and long-term losses. The global coefficient of variation c_{v_p} can be obtained according to 30, as follows:

$$c_{v_p} = \frac{\sqrt{\left(c_{v_F} \cdot \mu_F\right)^2 + \left(c_{v_{losses\_lt}} \cdot \mu_{losses\_lt}\right)^2 + \left(c_{v_{losses\_st}} \cdot \mu_{losses\_st}\right)^2}}{\mu_F + \mu_{losses\_lt} + \mu_{losses\_st}} \quad (20)$$

where c_{v_F} and μ_F are the coefficient of variation and the mean value of initial prestressing force, respectively; $c_{v_{losses\_lt}}$ and μ_{losses_lt} are , the coefficient of variation and the mean value of long-term prestress losses, respectively; $c_{v_{losses\_st}}$ and μ_{losses_st} are the immediate ones. All the coefficients of variation of Equation (20) have been obtained with reference to 31 and they have been assumed constants and equal to their mean values. For the application of the safety format, the equivalent cable of the post-tensioned system is adopted.

Table 1. Probability distributions of the basic variables and related design parameters.

Basic variables	Distribution type	Distribution parameters μ, c_v	Parameter references	Design parameters
f_c	Log-Normal	$f_{cm} = R_{ck,op} \cdot 0.83 + 8$ [MPa] $c_v = 0.10$	25 32	$f_{cd} = \frac{f_{ck}}{\gamma_c} = 21.7$ [MPa]
f_{up}	Log-Normal	$f_{upm} = f_{uk,op} \cdot 1.04$ [MPa] $c_v = 0.025$	31 31	$f_{upd} = \frac{f_{upk}}{\gamma_s} = 1475$ [MPa]
f_{ys}	Log-Normal	$f_{yms} = f_{yk,op} + 2 \cdot 30$ [MPa] $c_v = 0.025$	31 31	$f_{ysd} = \frac{f_{ysk}}{\gamma_s} = 305.6$ [MPa]
A_p (single strand)	Log-Normal	$A_{pm} = A_{pm,op}$ $c_v = 0.02$	12 33	$A_{pm} = 12.32$ [cm²]
P_{pt}	Log-Normal	$P_{ptm} = P_{pti,op} - \Delta P_{pt}$ $c_{v_p} = 0.08$	Equation (20)	$P_{ptm} = 1221.81$ [kN] (mid-span)

Once the parameters $\boldsymbol{\vartheta}_d$ are obtained, the safety ratios y_d for the perfect knowledge scenario can be determined and they are equal to:

- $y_{d,s} = V_{rd}/V_{ed} = 0.97$
- $y_{d,b} = M_{rd}/M_{ed} = 1.09$
- $y_d = \min(y_{d,s}, y_{d,b}) = 0.97$

4.3. Partial Knowledge Assessment

The partial knowledge scenario refers to a condition in which only a reduced number of tests is carried out, and a variability of $\overline{\boldsymbol{\vartheta}}_d$ arises due to the uncertain estimation of basic variables. Such a scenario is simulated starting from the probability distribution $f_X(\boldsymbol{x})$ of the random variables $\boldsymbol{X}$, and from the fixed number of tests n chosen. Many test campaigns involving the same number of tests

Preprints.org (www.preprints.org) | NOT PEER-REVIEWED | Posted: 6 March 2024 doi:10.20944/preprints202403.0290.v1

are simulated; each simulation, composed by a different set of samples, leads to a different estimation of the probability distribution of the parameters, given the confidence factor α, and consequently to different values $\bar{\boldsymbol{\vartheta}}_d$ of the estimated r.v. $\bar{\boldsymbol{\Theta}}_d$. From the latter, a probability distribution of the estimated safety ratio $\bar{Y}_d$ follows (Figure 5) and the properties of this distribution can be studied in order to evaluate the reliability of the method. It is interesting, indeed, to evaluate the probability that the estimated value $\bar{y}_d$ is lower than the reference value y_d. This probability is equal to the value assumed by the Cumulative Density Function (*CDF*) at the reference value, $F_{\bar{Y}_d}(y_d)$ or, equivalently, the area under the function $f_{\bar{Y}_d}(y_d)$ evaluated on the domain $\bar{y}_d < y_d$ (Figure 5).

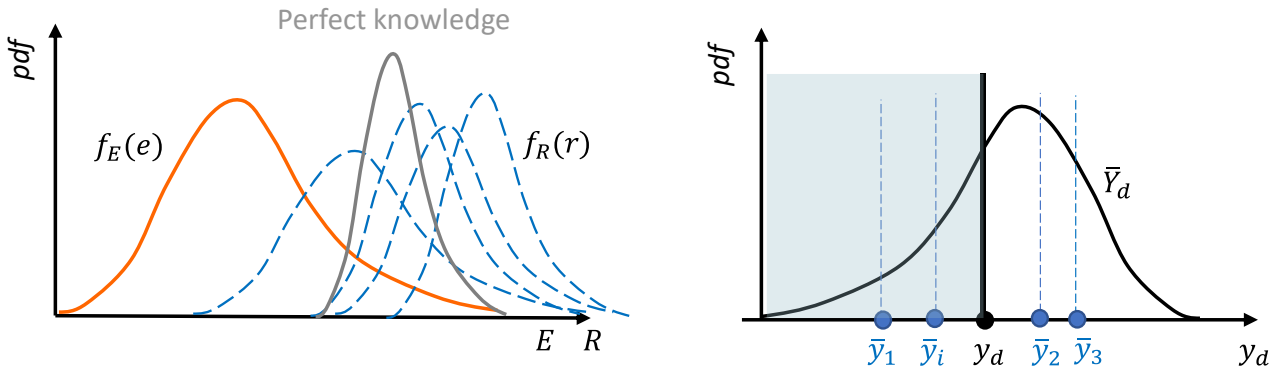

Figure 5. Safety assessment based on a partial knowledge.

The parameters are estimated through the recommendations contained in 12 following the condition of unknown variance σ of the basic variable distributions.

The characteristic values of the materials (f_{ck}, f_{ysk}, f_{upk}) are calculated through the Coverage Method 34. The characteristic value is obtained from the following formula:

$$\bar{f}_k = m - k_p \cdot s \tag{21}$$

where $\bar{f}_k$ is the estimated characteristic value, m is the sample mean, s is the sample standard deviation, and k_p is the estimation coefficient, calculated in Equation (22) and depending on the probability p corresponding to the desired k-percentile f_k, on the confidence level α, and on the sample size n.

$$k_p(p, \alpha, n) = -t(p, \alpha, n)/\sqrt{n} \tag{22}$$

where $t(p, \alpha, n)$ is the α-percentile of the generalised noncentral t-Distribution 36, corresponding to the probability p and with $n - 1$ degrees of freedom.

The mean values of the wires area (A_{pm}) and of the prestressing force P_{pt_m}, derived from samples, are estimated using the t-Student method 22 adopting the case of no prior information about the variable. The estimation of the mean value is obtained from the following formula:

$$\bar{X}_m = m + t_\alpha \frac{s}{\sqrt{n}} \tag{23}$$

where $\bar{X}_m$ is the estimation of the mean value, m and s are the mean and the standard deviation of the sample, n is the number of samples, and t_α is the percentile of the t-Distribution with degree of freedom $n - 1$ corresponding to a confidence level α.

By increasing the number of tests, the parameter estimation improves, and the sample distribution approximates better and better the probability density function of the population.

Once the parameters $\bar{\boldsymbol{\vartheta}}_d$ have been calculated, it is possible to carry out the safety checks and to obtain the safety measure $\bar{y}_d$. A Monte Carlo simulation 22 is applied to obtain the probability distribution of the safety ratio $\bar{Y}_d$. With the aim at evaluating how much uncertainties on the design parameters affect the estimated $\bar{y}_d$, the probability to stay into the safe domain $\bar{y}_d < y_d$ is calculated.

Preprints.org (www.preprints.org) | NOT PEER-REVIEWED | Posted: 6 March 2024 doi:10.20944/preprints202403.0290.v1

4.4. Assessment through Tests with Measurement Error Scenario

In this scenario, the $\bar{\boldsymbol{\vartheta}}_d$ are obtained in a similar way, but in this case the measurement error is also considered. According to the paragraph 3.3, the error is added to each sample value, by considering a probability distribution of the erroneous measurement having a coefficient of variation $c_{v,\varepsilon}$ and a mean value equal to the one of the samples itself.

5. Parametric Analysis and Related Results

This section presents the evaluation of the safety ratio y_d and its variability in the two scenarios simulating the performance of experimental campaigns.

In both scenarios, different analyses have been carried out by choosing different number n of tests and by exploring the α range [0.50-0.95] with the aim of observing how $F_{\bar{Y}_d}(y_d)$ changes. The following hypotheses have been assumed in the parametric analysis: in the first scenario, the same values of n and α are assumed for all the parameters $\bar{\boldsymbol{\vartheta}}_d$ and no measurement error is considered. In the second scenario, the measurement error is added, by considering different values of the coefficient of variation c_{v_ε}.

5.1. Outcomes of the Assessment through Tests without Measurement Error

Such a scenario simulates a possible experimental campaign conducted on the case study without considering any measurement error. The results obtained are reported in Figure 6 and in Figure 7. Figure 6 shows the *pdf*s of the shear safety ratio $\bar{y}_{d,s}$, of the bending one $\bar{y}_{d,b}$, and the *pdf*s of their envelopes $\bar{y}_d$, obtained for different values of n and α. To make the comparison easier, for all the three safety ratios the nondimensional ratio $\bar{y}_d/y_d$ is reported. In this way, the value 1 is the boundary between estimations of the capacity/demand ratio higher or lower than the reference case of perfect knowledge.

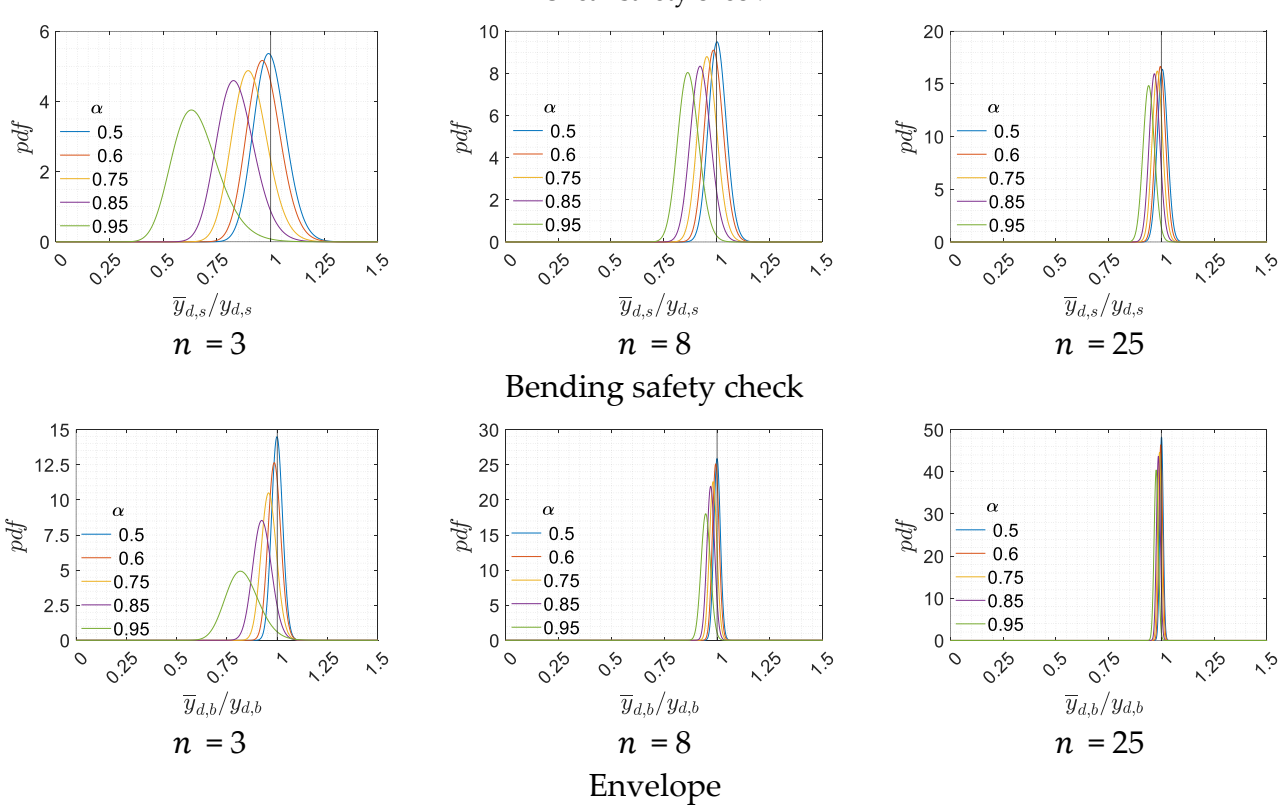

 doi:10.20944/preprints202403.0290.v1

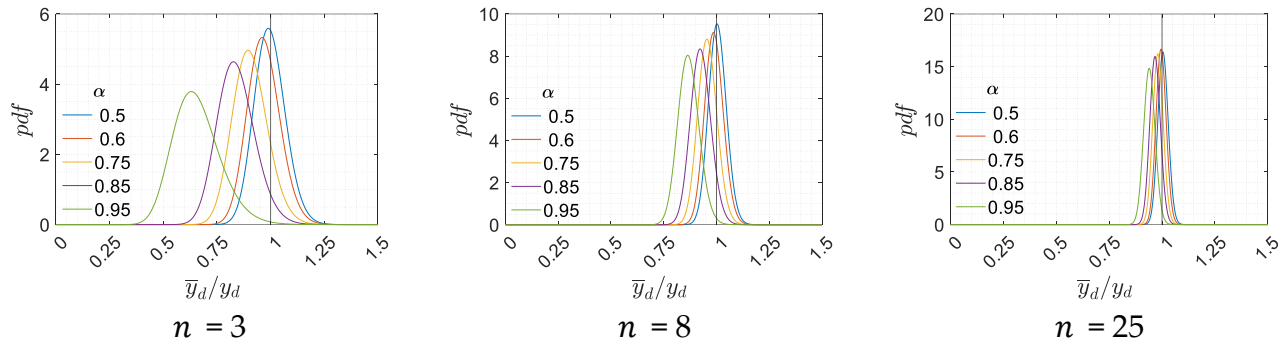

Figure 6. *pdf*s of the ratio $\bar{y}_d/y_d$, for different values of α and n.

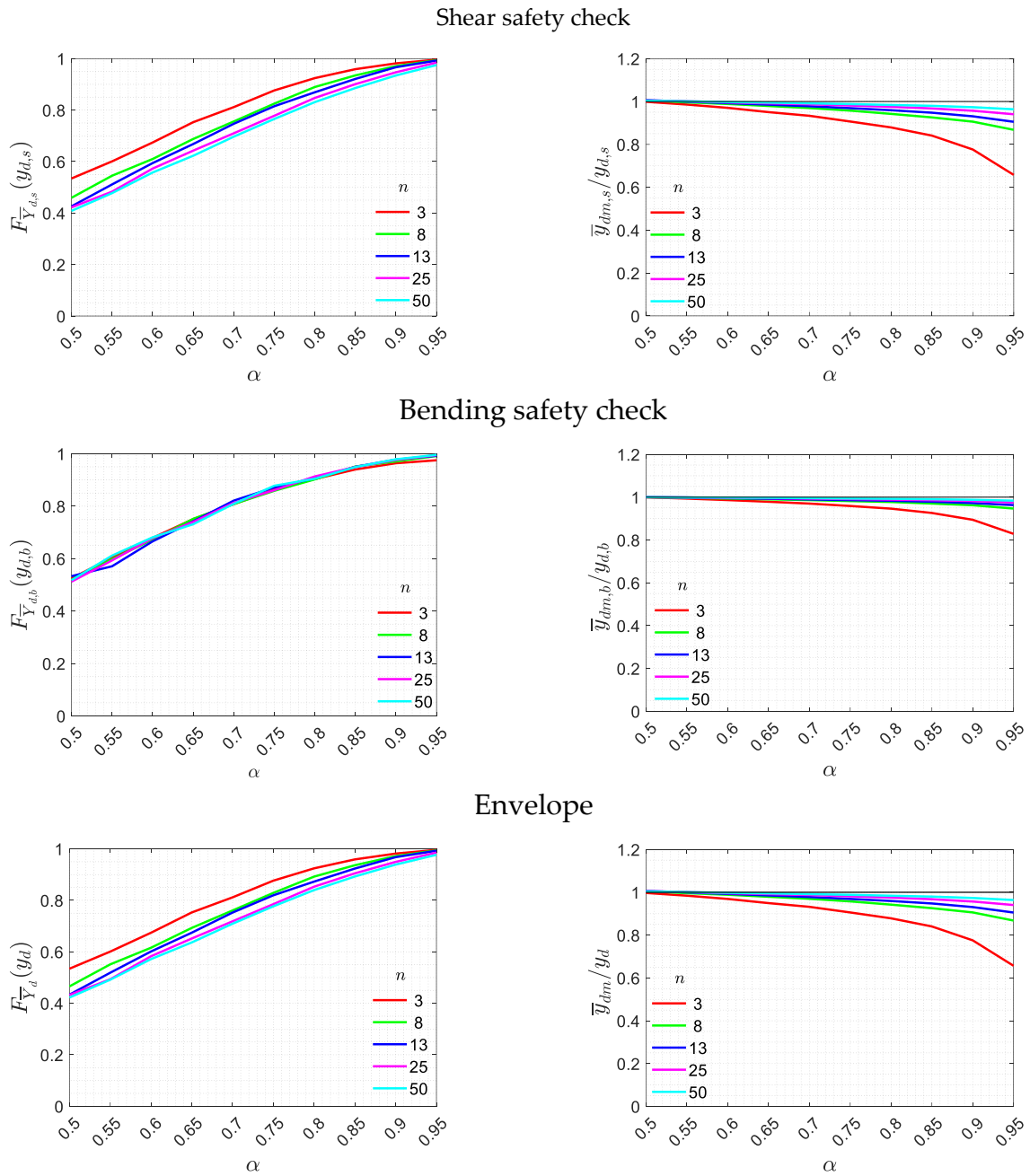

Figure 7. Diagrams of $F_{\bar{Y}_d}(y_d)$ and $\bar{y}_{dm}/y_d$ with α and n for shear, bending and envelope checks.

Preprints.org (www.preprints.org) | NOT PEER-REVIEWED | Posted: 6 March 2024 doi:10.20944/preprints202403.0290.v1

Figure 7 reports, instead, the trends of the *CDF* of $\bar{Y}_d$ evaluated at the reference value, $F_{\bar{Y}_d}(y_d)$, and of the mean value $\bar{y}_{dm} = E[\bar{Y}_d]$ in the nondimensional form, by varying the confidence level α and the number of tests n. It is important to underline that the choice of the partial factors do not affect the nondimensional reported results, since they appear both on $\bar{y}_d$ and y_d.

With the aim of understanding the results of this scenario in a clearer way, Tables 2, 4 and 6 display the numerical values obtained for the probability of estimating values of the safety ratio lower than the reference one $F_{\bar{Y}_d}(y_d)$, for the case of shear, bending, and envelope checks, while Tables 3, 5 and 7 contain the numerical results relevant to the ratio $\bar{y}_d/y_d$.

Table 2. Numerical values of $F_{\bar{Y}_{d,s}}(y_{d,s})$ for different values of α and n.

$F_{\bar{Y}_{d,s}}(y_{d,s})$		$\boldsymbol{\alpha}$				
		0.50	**0.60**	**0.75**	**0.85**	**0.95**
$\boldsymbol{n}$	**3**	0.53	0.67	0.87	0.95	0.99
	8	0.46	0.61	0.82	0.93	0.99
	25	0.42	0.57	0.78	0.99	0.99

Table 3. Numerical values of $\bar{y}_{dm,s}/y_{d,s}$ for different values of α and n.

$\bar{y}_{dm,s}/y_{d,s}$		$\boldsymbol{\alpha}$				
		0.50	**0.60**	**0.75**	**0.85**	**0.95**
$\boldsymbol{n}$	**3**	1	0.97	0.90	0.84	0.66
	8	1	0.99	0.96	0.92	0.87
	25	1	0.99	0.98	0.97	0.94

Table 4. Numerical values of $F_{\bar{Y}_{d,b}}(y_{d,b})$ for different values of α and n.

$F_{\bar{Y}_{d,b}}(y_{d,b})$		$\boldsymbol{\alpha}$				
		0.50	**0.60**	**0.75**	**0.85**	**0.95**
$\boldsymbol{n}$	**3**	0.52	0.68	0.86	0.94	0.98
	8	0.52	0.67	0.86	0.94	0.99
	25	0.51	0.68	0.86	0.95	0.99

 doi:10.20944/preprints202403.0290.v1

Table 5. Numerical values of $\bar{y}_{dm,b}/y_{d,b}$ for different values of α and n.

$\bar{y}_{dm,b}/y_{d,b}$		α				
		0.50	**0.60**	**0.75**	**0.85**	**0.95**
n	**3**	1	0.98	0.96	0.93	0.83
	8	1	0.99	0.98	0.97	0.95
	25	1	0.99	0.99	0.99	0.97

Table 6. Numerical values of $F_{\bar{Y}_d}(y_d)$ for different values of α and n.

$F_{\bar{Y}_d}(y_d)$		α				
		0.50	**0.60**	**0.75**	**0.85**	**0.95**
n	**3**	0.53	0.67	0.88	0.96	0.99
	8	0.47	0.62	0.83	0.94	0.99
	25	0.43	0.58	0.78	0.90	0.97

Table 7. Numerical values of $\bar{y}_{dm}/y_d$ for different values of α and n.

$\bar{y}_{dm}/y_d$		α				
		0.50	**0.60**	**0.75**	**0.85**	**0.95**
n	**3**	1	0.97	0.91	0.84	0.66
	8	1	0.99	0.96	0.93	0.87
	25	1	0.99	0.98	0.97	0.94

The results reported in the previous figures (Figures 6 and 7) and tables (Tables 2–7) are discussed first with reference to the different number of tests n, and successively by analysing the effect of variations of confidence α within the range considered.

Different choices on the number of tests n have a significant impact on the results obtained. By comparing the results of Figure 6 it is observed that by increasing the number of tests, the dispersion of the probability distributions reduces, and the mean value get closer to the reference scenario. This behaviour is expected as a higher number of tests leads to a better evaluation of the model uncertainties. On the other hand, by reducing n, the probability distributions move away from the reference scenario toward the safety zone (i.e. a capacity/demand ratio estimation lower than the reference scenario), but, at the same time, they are characterized by a greater standard deviation. Moreover, the shear dispersion is generally greater than the bending one. This aspect can be explained by the fact that the number of r.v. involved in $y_{d,b}$ is lower than the number of the r.v. involved in $y_{d,s}$. The different choices of n result in changes in the probability distributions, which in turn, affect the probability $F_{\bar{Y}_d}(y_d)$ of staying within the safety zone $\bar{y}_d < y_d$.

Preprints.org (www.preprints.org) | NOT PEER-REVIEWED | Posted: 6 March 2024 doi:10.20944/preprints202403.0290.v1

For what concerns the results for the shear check depicted in Figure 7 (first row), taking a low value of n leads to a larger, i.e. safer, value of $F_{\bar{Y}_{d,s}}(y_{d,s})$ and to a conservative value of $\bar{y}_{dm,s}/y_{d,s}$ because the methods used to calculate $\bar{\boldsymbol{\vartheta}}_d$ (see Equations (21) and (23)) produce conservative values of the estimated parameters thanks to the coefficient k_p, (see Equation (22)), and to the percentile t_α of the t-Distribution. This behaviour is also observed for the bending check (Figure 7) where the variation of n results in different values of $\bar{y}_{dm,b}/y_{d,b}$. As already observed in Figure 6, the different number of random variables involved in the estimation of $y_{d,b}$ has an effect also in the trends of the ratio $\bar{y}_{dm,b}/y_{d,b}$ of Figure 7, which are closer to each other with respect to those of the ratio $\bar{y}_{dm,s}/y_{d,s}$.

As expected, the choice of the confidence level α also produces different results. By increasing α, the mean value of the probability distributions (Figure 6) shifts to the left, providing an average value that is always smaller than the reference one. The safety check is statistically more precautionary, but at the same time, less accurate, since the dispersion increases, and a significant underestimation of the safety coefficient is likely to be obtained. The mean values reported in Figure 6 start from 1 for α equal to 0.5 and decrease in precautionary manner as α increases. This reduction is more pronounced with a small number of tests. At the same time, as already observed from the perspective of different n, the dispersion of the distribution $\bar{y}_d/y_d$ increases. This aspect negatively influences the probability $F_{\bar{Y}_d}(y_d)$ to obtain values of $\bar{y}_d$ lower than the reference value y_d. Once fixed α, the trend of $F_{\bar{Y}_d}(y_d)$ does not excessively change by varying the number n of tests. By assuming as a reference value the confidence level α equal to 0.75, as recommended by 12 and 34, the probability $F_{\bar{Y}_d}(y_d)$ is around 0.8 for different n and α (Figure 7).

5.2. Outcomes of the Assessment through Tests with Measurement Error

In addition to previous uncertainties related to test numbers and confidence factors, the current scenario also considers the impact of the measurement error on the safety assessment. Since in the literature there are no information about the measurement errors regarding tests for the survey of the prestressing system, in this work a credible coefficient of variation c_{v_ε} equal to 0.10 is assumed for the basic random variables selected in the previous sections. However, with the aim of providing a more general overview of the potential influence of this parameter for measurement systems more or less accurate than the previous ones, the main results have been also evaluated for different values of c_{v_ε}. In detail, results concerning $c_{v_\varepsilon} = 0.05$ and $c_{v_\varepsilon} = 0.20$ are reported and discussed at the end of this section.

The obtained results for c_{v_ε} equal to 0.10 are reported in Figures 8 and 9. Figure 8 shows the differences between the probability distribution with and without measurement error, depicted by solid and dashed lines, respectively, for the same values of n adopted in the previous section (Figure 6). The results are reported in term of shear, bending and envelope checks.

Shear safety check

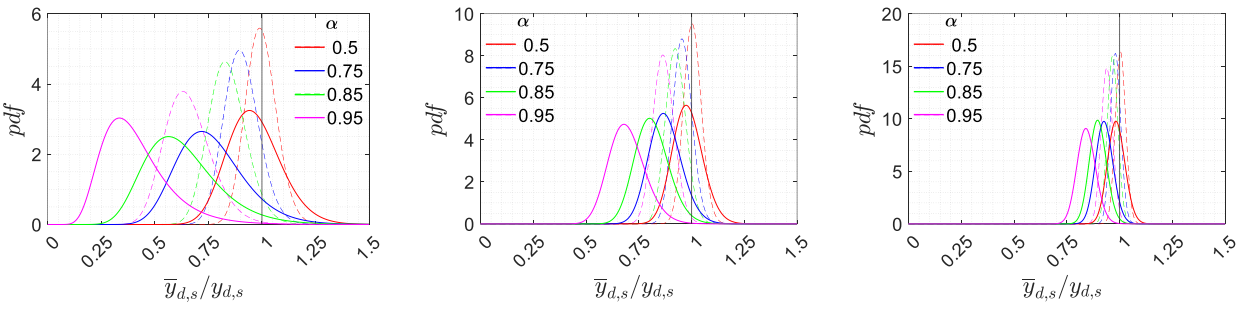

$n = 3$ $n = 8$ $n = 25$

Bending safety check

Preprints.org (www.preprints.org) | NOT PEER-REVIEWED | Posted: 6 March 2024 doi:10.20944/preprints202403.0290.v1

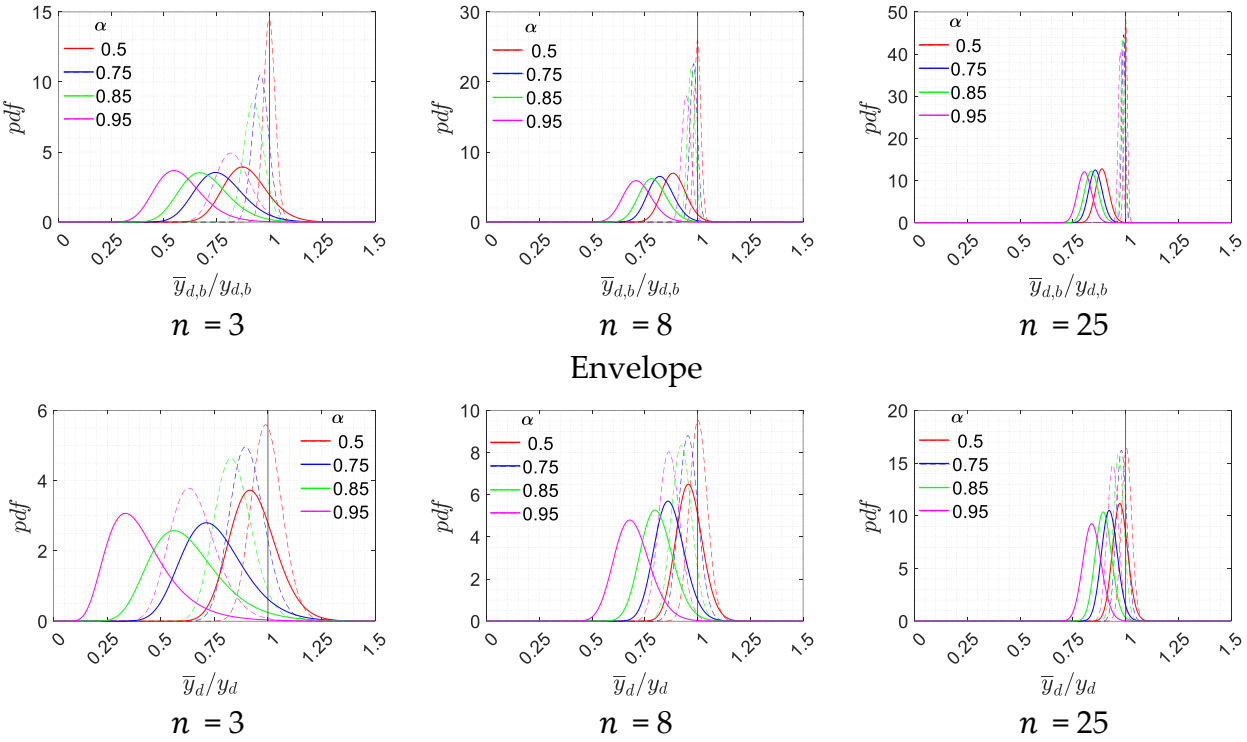

Figure 8. *pdf*s of the ratio $\bar{y}_d/y_d$, for different values of α and n by considering the measurement error.

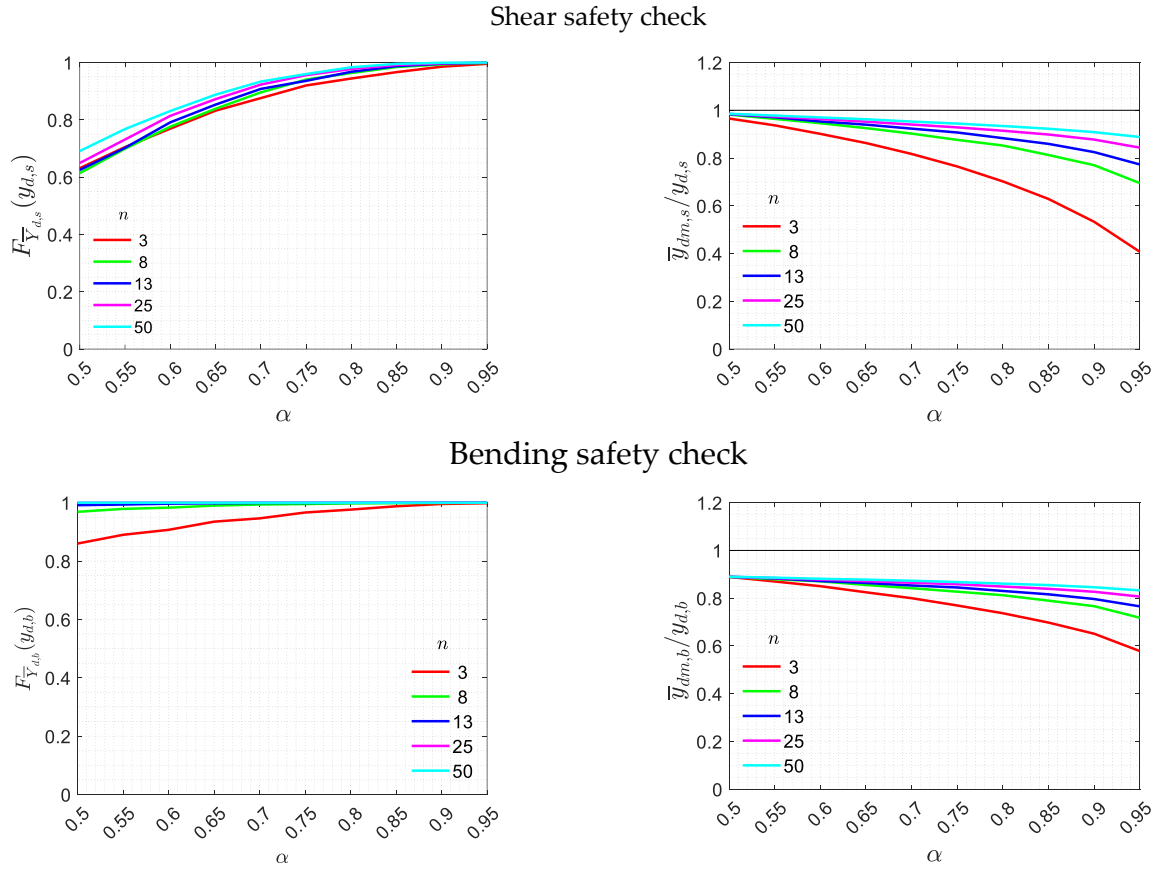

Preprints.org (www.preprints.org) | NOT PEER-REVIEWED | Posted: 6 March 2024 doi:10.20944/preprints202403.0290.v1

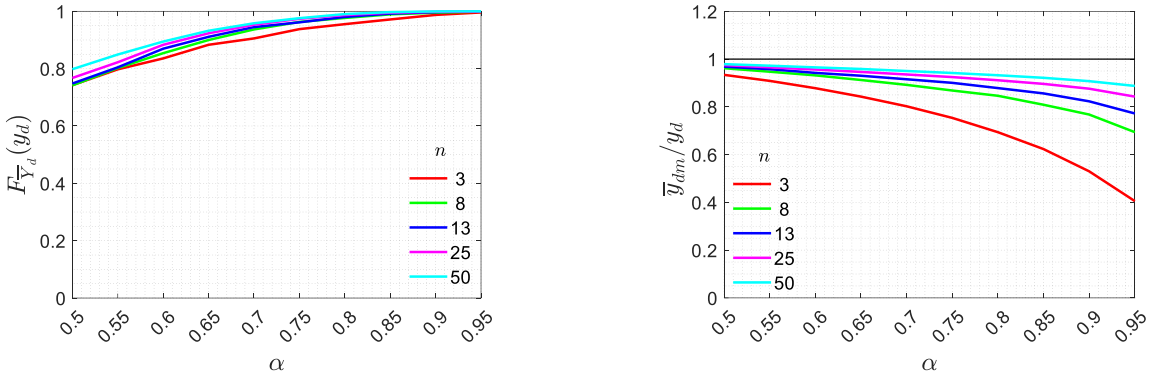

Figure 9. Diagram of $F_{\bar{Y}_d}(y_d)$ and $\bar{y}_{dm}/y_d$ with α and n for shear, bending and envelope checks.

Figure 9 reports the trends of $F_{\bar{Y}_d}(y_d)$ and the mean values $\bar{y}_{dm}$, obtained by varying n and α. Even in this scenario, the probability of obtaining a bending check worse than the shear check is low.

With the aim of understanding the results of this scenario in a clearer way, Tables 8, 10 and 12 display the numerical results for the shear, bending and envelope checks of $F_{\bar{Y}_d}(y_d)$, while Tables 9, 11, and 13 contain those related to $\bar{y}_d/y_d$.

Table 8. Numerical values of $F_{\bar{Y}_{d,s}}(y_{d,s})$ for different values of α and n with the measurement error.

$F_{\bar{Y}_{d,s}}(y_{d,s})$		$\boldsymbol{\alpha}$				
		0.50	**0.60**	**0.75**	**0.85**	**0.95**
$\boldsymbol{n}$	**3**	0.63	0.77	0.92	0.97	0.99
	8	0.61	0.78	0.94	0.98	0.99
	25	0.65	0.81	0.95	0.99	0.99

Table 9. Numerical values of $\bar{y}_{dm,s}/y_{d,s}$ for different values of α and n with the measurement error.

$\bar{y}_{dm,s}/y_{d,s}$		$\boldsymbol{\alpha}$				
		0.50	**0.60**	**0.75**	**0.85**	**0.95**
$\boldsymbol{n}$	**3**	0.96	0.90	0.76	0.63	0.40
	8	0.98	0.94	0.88	0.81	0.69
	25	0.98	0.96	0.93	0.89	0.84

Preprints.org (www.preprints.org) | NOT PEER-REVIEWED | Posted: 6 March 2024 doi:10.20944/preprints202403.0290.v1

Table 10. Numerical values of $F_{\bar{Y}_{d,b}}(y_{d,b})$ for different values of α and n with the measurement error.

$F_{\bar{Y}_{d,b}}(y_{d,b})$		α				
		0.50	**0.60**	**0.75**	**0.85**	**0.95**
n	**3**	0.89	0.93	0.97	0.99	1
	8	0.97	0.99	0.99	1	1
	25	1	1	1	15	1

Table 11. Numerical values of $\bar{y}_{dm,b}/y_{d,b}$ for different values of α and n with the measurement error.

$\bar{y}_{dm,b}/y_{d,b}$		α				
		0.50	**0.60**	**0.75**	**0.85**	**0.95**
n	**3**	0.89	0.85	0.77	0.70	0.58
	8	0.89	0.87	0.83	0.79	0.72
	25	0.89	0.87	0.86	0.84	0.81

Table 12. Numerical values of $F_{\bar{Y}_d}(y_d)$ for different values of α and n with the measurement error.

$F_{\bar{Y}_d}(y_d)$		α				
		0.50	**0.60**	**0.75**	**0.85**	**0.95**
n	**3**	0.75	0.83	0.93	0.97	0.99
	8	0.74	0.85	0.96	0.99	0.99
	25	0.77	0.88	0.97	0.99	0.99

Preprints.org (www.preprints.org) | NOT PEER-REVIEWED | Posted: 6 March 2024 doi:10.20944/preprints202403.0290.v1

Table 13. Numerical values of $\bar{y}_{dm}/y_d$ for different values of α and n with the measurement error.

$\bar{y}_{dm}/y_d$		α				
		0.50	**0.60**	**0.75**	**0.85**	**0.95**
n	**3**	0.93	0.88	0.75	0.62	0.41
	8	0.96	0.91	0.87	0.81	0.69
	25	0.98	0.96	0.92	0.89	0.84

The comparison depicted in Figure 8 shows that this additional uncertainty source shifts the probability distribution toward conservative $\bar{y}_d$ values. Given the same values of α and n, this translation is more pronounced with respect to the previous case (no measurement error) and the dispersion is larger. From the combination of these two factors, it follows that the probability $F_{\bar{Y}_d}(y_d)$ of obtaining values of $\bar{y}_d$ lower than the reference one is enhanced and the mean value $\bar{y}_{dm}$ reduces, with respect to the previous scenario. Similar trends are observed for all the values of α and n.

Aiming at observing how much the structural safety is affected by different measurement errors, the results for c_{v_ε} equal to 0.05 (Figure 10a) and 0.20 (Figure 10b) are reported only for $\bar{y}_{dm}/y_d$ relevant to the envelope case. Figure 10 shows that the measurement error significantly influences the final value of the estimated capacity mean $\bar{y}_{dm}$.

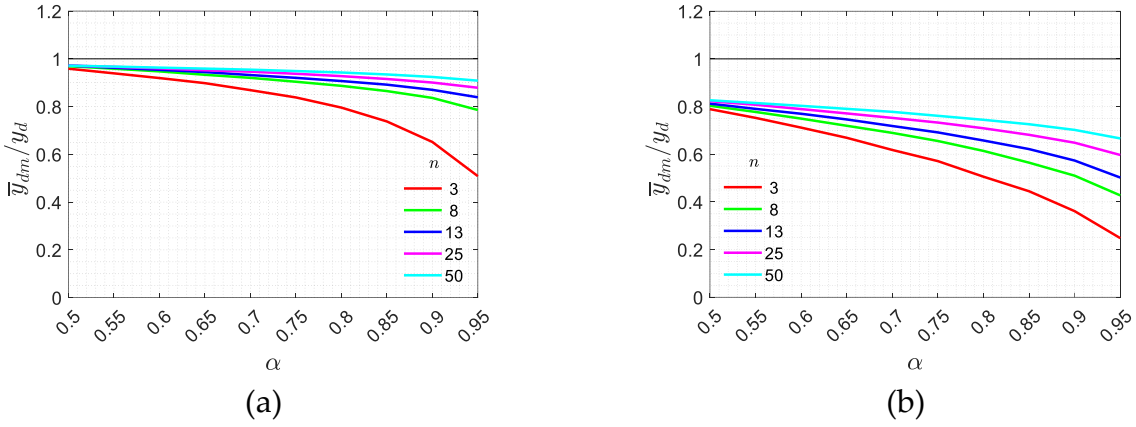

Figure 10. Diagram of $\bar{y}_{dm}/y_d$ related to the envelope check by varying α and n with measurement error equal to 0.05 (a) and 0.20 (b).

It is also worth to observe that, by increasing the measurement error variability, the probability to have a safe estimation of $\bar{y}_d$ increases. The uncertainty due to the measurement error introduces an extra variability of the measured quantity that implies a further safety on the final results. This is a remarkable difference between new structures and existing ones, and it should be considered within the safety format to avoid over-conservative safety assessments.

6. Conclusions

In this paper the uncertainties affecting the safety assessment based on the semi-probabilistic approach for existing post-tensioned prestressed bridges is studied. The knowledge process is simulated by the Monte Carlo method, and it is defined by (i) the number n of tests, (ii) the confidence level α used for the estimation of the design parameters, and (iii) the coefficient of variation c_{v_ε} of the measurement error. Some strengths and weakness of the safety format applied to this type of post-tensioned prestressed structures are highlighted in the following.

 doi:10.20944/preprints202403.0290.v1

- The safety format is robust since different levels of n and α lead almost always to a conservative estimation of the capacity/demand ratio. Namely the probability to obtain estimated safety ratios $\bar{y}_d$ lower than the reference value y_d is high and often close to 1. As expected, this probability increases by increasing the number of tests and the confidence level. For the value of confidence α equal to 0.75, recommended by the Eurocodes 12, the probability $F_{\bar{Y}_d}(y_d)$ to have a safety estimation of $\bar{y}_d$ is high in both the scenarios, with and without the measurement error.
- Results depend on the expressions used for the estimation of the design parameters $\bar{\boldsymbol{\vartheta}}_d$, and relevant underlying assumption. The Eurocode formulas, based on Coverage Method and t-Student method, provide satisfactory results.
- In the scenario that neglects the measurement error, high values of the confidence factor α, approximately larger than 0.8, do not notably improve the result $F_{\bar{Y}_d}(y_d)$, but significantly reduce the expected value $\bar{y}_{d,m}$ of $\bar{Y}_d$. Thus, it becomes very probable to obtain under-estimation of the safety ratio, and, in a misleading way, the structure could appear to be not adequate.
- Measurement error significantly influences the results. The safety format still provides conservative results, but the probability of under-estimate the structural capacity is more and more increased.

Presented results refer to a quite diffused girder typology, but they cannot be considered definitive, and the problem requires further investigations. Furthermore, a credible variability of the outcomes provided by the measurement errors has been considered (coefficient of variation equal to 0.1), but few studies exist about this topic, especially for what concerns tests and technologies for the estimation of the tensile force and strength of prestressing cable 37, as well as of the detrimental effects of corrosion 18.

References

1. Scozzese, F.; Minnucci, L. Seismic Risk Analysis of Existing Link Slab Bridges Using Novel Fragility Functions. Applied Sciences **2023**, *14*, 112. https://doi.org/10.3390/app14010112.
2. Minnucci, L.; Scozzese, F.; Carbonari, S.; Gara, F.; Dall'Asta, A. Innovative Fragility-Based Method for Failure Mechanisms and Damage Extension Analysis of Bridges. Infrastructures **2022**, *7*, 122. https://doi.org/10.3390/infrastructures7090122.
3. Ragni, L.; Scozzese, F.; Gara, F.; Tubaldi, E. Dynamic Identification and Collapse Assessment of Rubbianello Bridge.; Guimarães, Portugal, 2019; pp. 619–626.
4. COST 345. Procedures for the assessment of Highway Structures. Final Report, Reports of Working Groups 1-6. 2004
5. Zhang, W.; Wang, N. Bridge Network Maintenance Prioritization under Budget Constraint. Structural Safety **2017**, *67*, 96–104. https://doi.org/10.1016/j.strusafe.2017.05.001.
6. Frangopol, D.M. Life-Cycle Performance, Management, and Optimisation of Structural Systems under Uncertainty: Accomplishments and Challenges [1]. Structure and Infrastructure Engineering **2011**, *7*, 389–413. https://doi.org/10.1080/15732471003594427.
7. Pinto, P.E.; Franchin, P. Issues in the Upgrade of Italian Highway Structures. Journal of Earthquake Engineering **2010**, *14*, 1221–1252. https://doi.org/10.1080/13632461003649970.
8. Federal Highway Administration-HRT-13-028: Guidelines for Sampling, Assessing, and Restoring Defective Grout in Prestressed Concrete Bridge Post-Tensioning Duts. 2013
9. Highways England. CS 465 Management of Post-Tensioned Concrete Bridges. 2020
10. Highways England. CS 464 Non-destructive testing on highways structures. 2020
11. Italian Ministry of Infrastructures and Transport, Decree 01/07/2022, n. 204, Guidelines on Risk Classification and Management, Safety Assessment and Monitoring of Existing Bridges, Italian Minestry of Infrastrucures and Transport: Rome, Italy, 2020.
12. CEN EN 1990 Eurocode 0- Basis of Structural Design. CEN 2002, Brussels
13. fib. Bullettin N°80. Partial Safety factor Methods for Existing Structures, Lausanne. 2016
14. Gino, D.; Castaldo, P.; Bertagnoli, G.; Giordano, L.; Mancini, G. Partial Factor Methods for Existing Structures According to Fib Bulletin 80: Assessment of an Existing Prestressed Concrete Bridge. Structural Concrete **2020**, *21*, 15–31. https://doi.org/10.1002/suco.201900231.

15. Lara, C.; Tanner, P.; Zanuy, C.; Hingorani, R. Reliability Verification of Existing RC Structures Using Partial Factors Approaches and Site-Specific Data. Applied Sciences **2021**, *11*, 1653. https://doi.org/10.3390/app11041653.
16. Frangopol, D.M.; Kim, S. Service Life, Reliability and Maintenance of Civil Structures. In Service Life Estimation and Extension of Civil Engineering Structures; Elsevier, 2011; pp. 145–178 ISBN 978-1-84569-398-5.
17. Cesare, M.A.; Santamarina, C.; Turkstra, C.; Vanmarcke, E.H. Modeling Bridge Deterioration with Markov Chains. J. Transp. Eng. **1992**, *118*, 820–833. https://doi.org/10.1061/(ASCE)0733-947X(1992)118:6(820).
18. Ma, Y.; Zhang, J.; Wang, L.; Liu, Y. Probabilistic Prediction with Bayesian Updating for Strength Degradation of RC Bridge Beams. Structural Safety **2013**, *44*, 102–109. https://doi.org/10.1016/j.strusafe.2013.07.006.
19. Vereecken, E.; Lombaert, G.; Caspeele, R. Bayesian Assessment of the Remaining Prestressing Reinforcement in Existing Concrete Bridges. In fib symposium proceedings **2021**, 1386-1397
20. Caspeele, R.; Taerwe, L. Influence of Concrete Strength Estimation on the Structural Safety Assessment of Existing Structures. Construction and Building Materials **2014**, *62*, 77–84. https://doi.org/10.1016/j.conbuildmat.2014.03.033.
21. Paté-Cornell ME. Uncertainties in risk analysis: Six levels of treatment. Reliability Engineering & System Safety **1996**; 54, 95–111. https://doi.org/10.1016/S0951-8320(96)00067-1.
22. Ang AH-S, Tang WH, Ang AH-S. Probability Concepts in Engineering: Emphasis on Applications in Civil & environmental Engineering, 2nd ed; Wiley, New York, **2007**.
23. Huber, P.; Huber, T.; Kollegger, J. Experimental and Theoretical Study on the Shear Behavior of Single- and Multi-span T- and I-shaped Post-tensioned Beams. Structural Concrete **2020**, *21*, 393–408. https://doi.org/10.1002/suco.201900085.
24. Herbrand M, Kueres D, Classen M, Hegger J. Experimental Investigations on the Shear Capacity of Prestressed Concrete Continuous Beams with Rectangular and I-Shaped Cross-Sections. In: Hordijk DA, Luković M, editors. High Tech Concrete: Where Technology and Engineering Meet, Cham: Springer International Publishing; **2018**, p. 658–66. *https://doi.org/10.1007/978-3-319-59471-2_78*.
25. Italian Ministry of Infrastrucutures and Transport. Decree 17/01/2018, n.42. Adjournament of << Technical Code for Constructions>>; Italian Ministry of Infrastructures and Transports: Rome, Italu, **2018**
26. CEN EN 1992-1 Eurocode 2- Design of Concrete Structures, Part1: CEN 2005. Brussels
27. Birgin, H.B.; Laflamme, S.; D'Alessandro, A.; Garcia-Macias, E.; Ubertini, F. A Weigh-in-Motion Characterization Algorithm for Smart Pavements Based on Conductive Cementitious Materials. Sensors **2020**, *20*, 659. https://doi.org/*10.3390/s20030659*.
28. CEN EN 1991. Eurocode 1 – Actions on Structures, CEN **2005**. Brussels
29. CSI. SAP200. Computers and Structures Inc. Berkley, CA.
30. Lemons, D.S.; Langevin, P. An Introduction to Stochastic Processes in Physics: Containing "On the Theory of Brownian Motion" by Paul Langevin, Translated by Anthony Gythiel; Johns Hopkins University Press: Baltimore, **2002**; ISBN 978-0-8018-6866-5.
31. Joint Committee on Structural Safety. JCSS Probabilistic Model Code, Part 3: Resistance Models. **2002**
32. Wisniewski D.F. Safety Formats for the Assessment of Concrete Bridges. **2007**
33. CEN. EN 10138-2. Prestressing Steels – Part 2: Wire. **2000** Brussels
34. Leonardo da Vinci Pilot Project CZ/02/B/F/PP-134007. Handbook 2. Reliability Backgrounds, Guide to the basis of structural reliability and risk engineering related to Eurocodes, supplemented by practical example. **2005**
35. Holický M, Vorlíček M. Statistical Procedures for Design Assisted by Testing **1996**; https://doi.org/10.5169/SEALS-56082.
36. Owen, D.B. A Survey of Properties and Applications of the Noncentral T-Distribution. Technometrics **1968**, *10*, 445. https://doi.org/*10.2307/1267101*.
37. Morelli, F.; Panzera, I.; Piscini, A.; Salvatore, W.; Chichi, F.; Marconi, G.; Maestrini, D.; Gammino, M.; Mori, M. X-Ray Measure of Tensile Force in Post-Tensioned Steel Cables. Construction and Building Materials **2021**, *305*, 124743. https://doi.org/*10.1016/j.conbuildmat.2021.124743*.